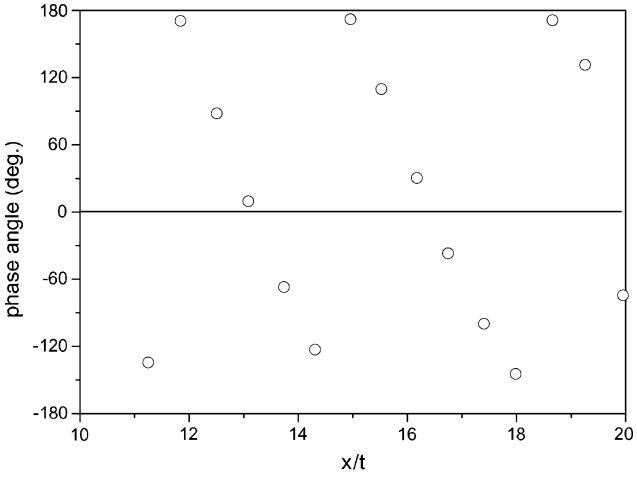

Fig. 6 Phase angle, $c/t = 10$, $Re = 300$.

vortex shedding from rectangular plates[1,2,5] m in Eq. (4) is related to the number of vortices formed on the plate's side or to the multiwave solutions of the problem. In Figs. 5 and 6 we show the phase angle ϕ of the velocity oscillations at the dominant frequency along the plate's side. The phase angle, relative to the reference point at the leading edge ($x = 0$), is computed at a distance of about $0.5t$ from the plate's side. The dominated frequency has been detected using the fast Fourier transform. We used a bandpass filter when more than one frequency exists. We found that the vortex shedding frequency in the wake is equal to the dominated frequency computed along the plate's side. The data in Figs. 5 and 6 show that $\phi = 2\pi mx/c$, which supports our travel-wave assumption (2) regarding the wavelength. The same result has been measured by Nakamura et al.[2] at Reynolds numbers $(1–3) \times 10^3$.

Conclusions

Experimental studies of vortex shedding from a rectangular elongated plate, when the cord length parallel to the flow (c) is much greater than its height (t), show that the Strouhal number $Sr(c)$ increases stepwise with c/t increasing from 3 to 12. Investigating a flow phenomenon described by a frequency f, one can consider a Strouhal number $Sr = fl/u$ as a nondimensional frequency when l and u are characteristic length and velocity, respectively. For a phenomenon considered in this Note, $l = c/m$ and $u \approx 0.5–0.6U$ are a natural choice for characteristic parameters, when m and U are the number of vortices (bubbles) formed on the plate's side and the freestream velocity, respectively. This was confirmed numerically for Reynolds numbers $Re = Ut/\nu > 300$. Assuming that vortex shedding has a traveling-wave nature, we suggest simple considerations for explaining the trend of the Strouhal number to increase stepwise.

Acknowledgments

This research was supported by Israel Science Foundation Grant 159/02 and in part by CEAR of the Hebrew University of Jerusalem. The work of N.N. was also supported in part by the Russian Foundation for Basic Research under Grant 02-01-00492. A.Y. thanks A. Eidelman for useful discussions.

References

[1]Nakamura, Y., and Nakashima, M., "Vortex Excitation of Prisms with Elongated Rectangular, H and ⊢ Cross-Sections," *Journal of Fluid Mechanics*, Vol. 163, 1986, pp. 149–169.

[2]Nakamura, Y., Ohya, Y., and Tsuruta, H., "Experiments on Vortex Shedding from Flat Plates with Square Leading and Trailing Edges," *Journal of Fluid Mechanics*, Vol. 222, 1991, pp. 437–447.

[3]Rockwell, D., and Naudascher, E., "Review of Self-Sustaining Flow past Cavities," *Journal of Fluids Engineering*, Vol. 100, 1978, pp. 152–165.

[4]Hourigan, K., Thompson, M. C., and Tan, B. T., "Self-Sustained Oscillations in Flows Around Long Blunt Plates," *Journal of Fluids and Structures*, Vol. 15, 2001, pp. 387–398.

[5]Nakamura, Y., Ohya, Y., Ozono, S., and Nakayama, R., "Experimental and Numerical Analysis of Vortex Shedding from Elongated Rectangular Cylinders at Low Reynolds numbers $200–10^3$," *Journal of Wind Engineering and Industrial Aerodynamics*, Vol. 65, 1996, pp. 301–308.

[6]Ohya, Y., Nakamura, Y., Ozono, S., Tsuruta, H., and Nakayama, R., "A Numerical Study of Vortex Shedding from Flat Plates with Square Leading and Trailing Edges," *Journal of Fluid Mechanics*, Vol. 236, 1991, pp. 445–460.

[7]Kim, J., Kim, D., and Choi, H., "An Immersed-Boundary Finite-Volume Method for Simulations of Flow in Complex Geometries," *Journal of Computational Physics*, Vol. 171, 2001, pp. 132–150.

H. Reed
Associate Editor

Study of Flame Structure and Soot Formation on Heptane/Air Diffusion Flame

Xuelei Zhu*
Fluent, Inc., Lebanon, New Hampshire 03766-1442
and
Jay P. Gore†
Purdue University, West Lafayette, Indiana 47907-1003

Introduction

HIGHER hydrocarbon fuels are extensively used in practical devices such as internal combustion engines, industrial furnaces, and powerstation gas turbines. Normal heptane (n-C_7H_{16}) is a representative higher hydrocarbon fuel. The laminar flame speed of n-heptane/air[1] and the structure of opposed flow heptane flames[2,3] have been studied experimentally and numerically. Many gaseous species, up to C_6-hydrocarbon, were measured, and the numerical results showed relatively good agreement with the measurements, except for the higher hydrocarbon species. A chemical mechanism for n-heptane oxidation and pyrolysis has been developed and validated against several independent data sets, including flow reactor experiments by Held et al.[4] A few other heptane chemical mechanisms have been also reported.[5,6] The soot formation in heptane flames has been studied by the use of global soot kinetics[7,8]; however, a global gas chemical mechanism for heptane combustion was used in this study.

The soot formation and soot radiation effects in heptane flames, especially in high-pressure flames, have not yet been studied by consideration of detailed gas chemical kinetics and full treatment of radiation heat loss. The soot and radiation effects in opposed flow methane/air diffusion flames were studied previously.[9] The radiation heat loss with both emission and absorption is considered with the exact solution of the radiation transfer equation for a nongray medium. The radiation from soot strongly affects the soot formation.

The specific objective of this Note is to study the opposed flow heptane/air diffusion flame structure, including soot formation, by the use of different detailed gas chemical mechanisms and global soot kinetics, as well as different thermal radiation models. The calculations that used different heptane mechanisms were compared with the measurements by Seiser et al.[2] for temperature and species distributions.

Received 10 February 2004; revision received 8 April 2004; accepted for publication 12 April 2004.

*Computational Fluid Dynamics Engineer, 10 Cavendish Court; xz@fluent.com. Senior Member AIAA.

†Professor, School of Mechanical Engineering. Associate Fellow AIAA.

Computational Method

The calculations were performed with the Sandia National Laboratories OPPDIF code,[10] modified by the addition of a soot kinetics formulation and a radiation model. Two different heptane mechanisms, Held's kinetics[4] and University of Utah kinetics,[11] were used with their accompanying thermochemical data. Held's kinetics contains 275 elementary reactions involving 41 chemical species, up to C_7H_{16}, without polycyclic aromatic hydrocarbon (PAH) species, for n-heptane oxidation and pyrolysis reactions. The University of Utah kinetics is much more complicated, containing 848 elementary reactions with 180 chemical species, with up to four aromatic rings, PAH species, and pyrene. This kinetic mechanism is composed of heptane, iso-octane and PAH formation submechanisms.

The opposed flow heptane/air diffusion flame were chosen as follows to match the experimental conditions.[2] The injection velocities of the mixture of prevaporized n-heptane and N_2($X_F = 0.15$, $X_{N2} = 0.85$) and air were set to 0.342 and 0.375 m/s, and the fuel and air temperatures were set at 338 and 298 K, respectively.

The soot formation is simulated with Lindstedt's global soot kinetics model (see Ref. 12). This soot kinetics was used for methane flames,[9] acetylene flames,[13] and heptane flames.[8] Good agreement was found between experimental data and predictions. By the use of this soot kinetic model, the OPPDIF code was modified to include the equations of soot mass fraction and soot particle number density. It has been shown that soot oxidation due to the OH radical is important.[9] In this study, the additional OH oxidation term was also considered, as well as the thermophoretic effects. The gaseous species (C_2H_2, OH, O_2, CO, and H_2) production and consumption rates due to the soot reactions were rigorously accounted for in the gas-phase conservation equations. The details are fully discussed in Ref. 9.

Radiation Model

Three different treatments of gaseous molecule and soot particle radiation heat loss were considered: adiabatic, an emission approximation, and an exact solution that included emission and absorption of radiation. The emission approximation for gas species[14] and soot particles[13] are fully discussed in Ref. 13 and 14, respectively.

The radiation source term that considers both gas emission and absorption is calculated with the exact solution of the radiation transfer

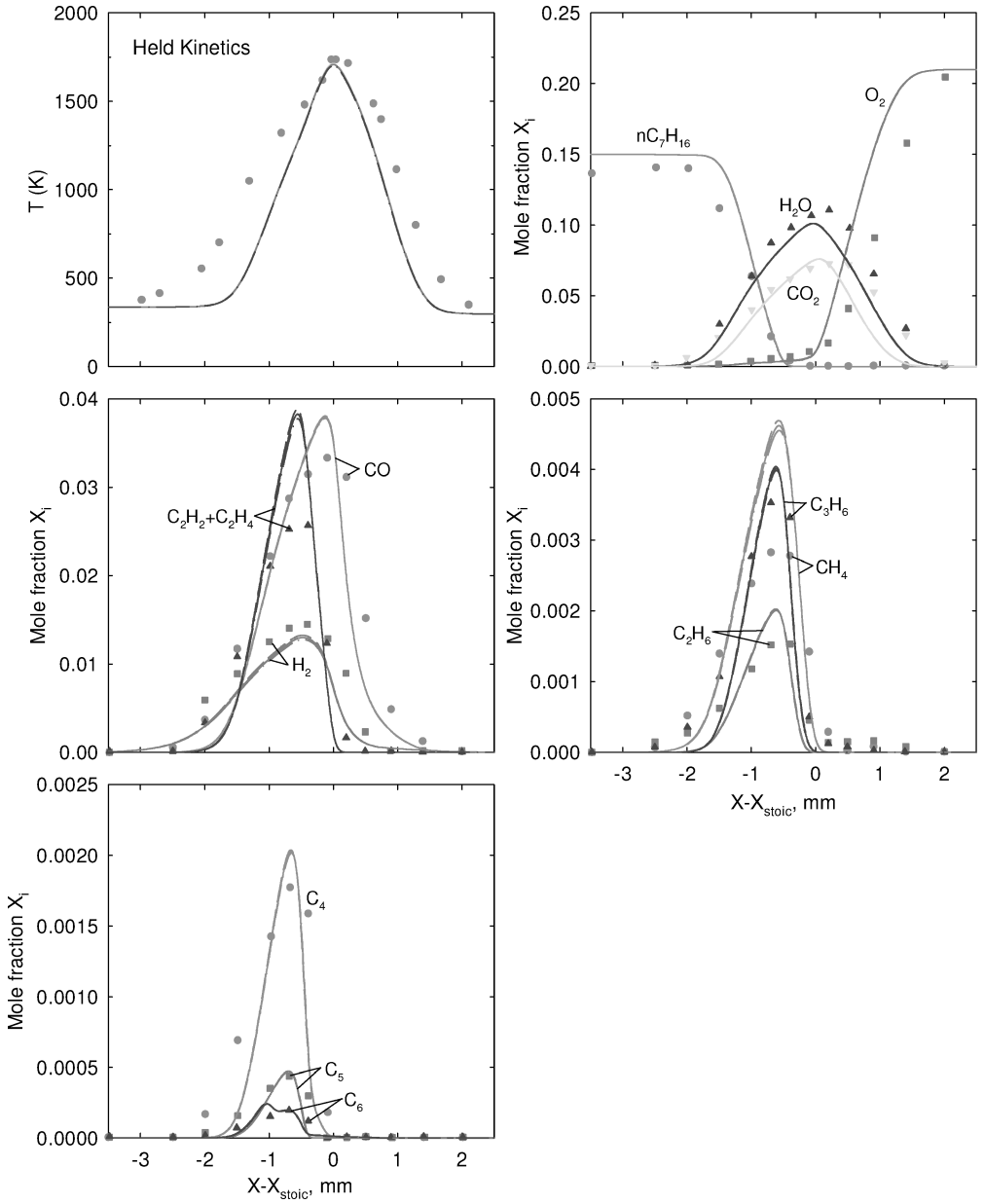

Fig. 1 Temperature and species mole fractions predicted by Held's kinetics for heptane/air diffusion flame; measured (symbols) and calculated: – – –, adiabatic; ——, emission/absorption; and –·–, emission curve profiles plotted as a function of distance from stoichiometric position.

equation for a nongray medium with cold walls, given by Crosbie and Viskanta[15]:

$$Q_{\text{rad}}(x) = 2\pi \sum_{i}^{M} k_i(x) \left\{ \int_0^x k_i(x') I_b(x') W_i(x') E_1[k_i(x - x')]\, \mathrm{d}x' + \int_x^L k_i(x') I_b(x') W_i(x') E_1[k_i(x' - x)]\, \mathrm{d}x' - 2I_b(x) W_i(x) \right\} \tag{1}$$

The two integral terms on the right-hand side represent the absorption of radiation at the location x that originates from the location x'. The third term on the right-hand side represents the emission from the location x. L is the distance between the fuelstream and the airstream, $E_n(x)$ are the nth exponential integral functions, I_b is the wavelength integrated blackbody intensity, and M is the number of equivalent gray gases. The local emission coefficient is represented as the product of the gray gas absorption coefficient k_i in the ith band weighted by the Planck function weights $W_i(T)$.

The gas molecule spectral absorption coefficients k_i are calculated from the weighted sum of gray gases model (WSGGM)-based spectral model[16,17]:

$$k_i = k_{io}\left(P_{\text{abs}} / T^2\right) e^{-\alpha_i / T} \tag{2}$$

P_{abs} is the sum of the partial pressures of the absorbing/emitting gases. The absorption coefficient k_{io} and the exponential dependence coefficient on temperature α_i are calculated with minimization of the modeling error in comparison with a detailed narrowband model determined with RADCAL.

Like the gas radiation treatment, the radiation source term that considers both emission and absorption by the soot particles is calculated as

$$Q_{\text{rad}}(x) = 2\pi \int_0^{\infty} k_\lambda(x) \left\{ \int_0^x k_\lambda(x') I_{b\lambda}(x') E_1[k_\lambda(x - x')]\, \mathrm{d}x' + \int_x^L k_\lambda(x') I_{b\lambda}(x') E_1[k_\lambda(x' - x)]\, \mathrm{d}x' - 2I_{b\lambda}(x) \right\} \mathrm{d}\lambda \tag{3}$$

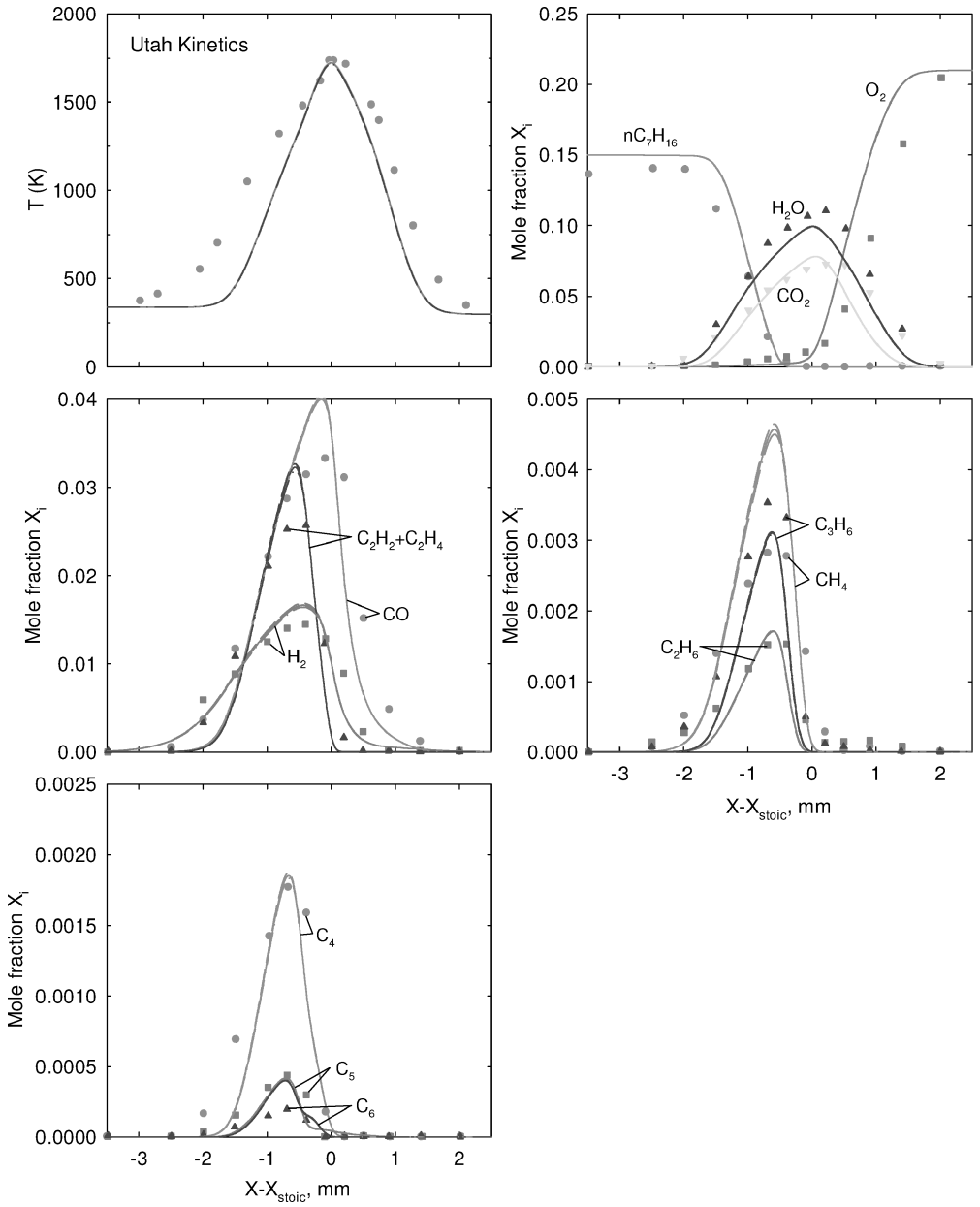

Fig. 2 Temperature and species mole fractions predicted by University of Utah kinetics for heptane/air diffusion flame; measured (symbols) and calculated: – – –, adiabatic; ——, emission/absorption; and –·–, emission curve profiles plotted as a function of distance from stoichiometric position.

The spectral absorption coefficient of a soot particle k_λ can be obtained by[18]

$$k_\lambda = C f_v / \lambda \tag{4}$$

where $C = 4.58$ is a constant, f_v is soot volume fraction, and λ is wave number.

Results and Discussion

Figure 1 shows a comparison of the experimental data (symbols) and predictions (curves) of temperature and species mole fractions (C_7H_{16}, O_2, H_2O, CO_2, CO, H_2, CH_4, $C_2H_2 + C_2H_4$, C_2H_6, C_3H_6, C_4, C_5, C_6) by the use of Held's heptane kinetics. All of the profiles are plotted as a function of the distance from the stoichiometric point, which is defined as the peak temperature location. Matching the flame location can remove the effects of differences in the peak temperature location between predictions and experiments,[2] which is about 0.3 mm at the current condition. The three radiation condition cases, adiabatic, emission only, and emission/absorption, are shown and compared. The radiation effects on temperature and species, except for CH_4 and $C_2H_2 + C_2H_4$, are not very strong for the present flame conditions. Both temperature and major species profiles show reasonable agreement. The minor species (CH_4, $C_2H_2 + C_2H_4$, C_2H_6, and C_3H_6) calculations show an overestimation compared to the measurements, especially for CH_4 and $C_2H_2 + C_2H_4$ species. The concentrations of C_2H_2 and C_2H_4 are roughly of the same order of magnitude at the present flame condition. The only C_4-, C_5-, and C_6-hydrocarbons in Held's mechanism are C_4H_6, C_4H_8, C_5H_{10}, C_6H_6, C_6H_{10}, and C_6H_{12}. The calculations of higher hydrocarbons show reasonably good agreement with the measurements, except for the overprediction of C_4.

The temperature and the species mole fractions profiles determined by the University of Utah heptane kinetics are shown in Fig. 2. All of the profiles are plotted as functions of the distance from the flame sheet. The adiabatic, emission only, and emission/absorption radiation cases are compared. The results show good agreement for major species and temperature, similar to that shown in Fig. 1. The University of Utah kinetics significantly improves the prediction of higher hydrocarbon species concentrations (above the C_2-hydrocarbons) compared to the calculations by Held's kinetics. This is especially true for $C_2H_2 + C_2H_4$, C_2H_6, and C_4-hydrocarbon species. More detailed higher hydrocarbon reactions, including PAH formation, as well as more high hydrocarbon species, including 27 C_4-, 13 C_5-, 15 C_6-, and 68 over C_7- higher hydrocarbon species were considered in these kinetics. The summation of all of these C_4-, C_5-, and C_6-hydrocarbons are plotted in Fig. 2. The higher hydrocarbon species can be predicted more accurately by the inclusion

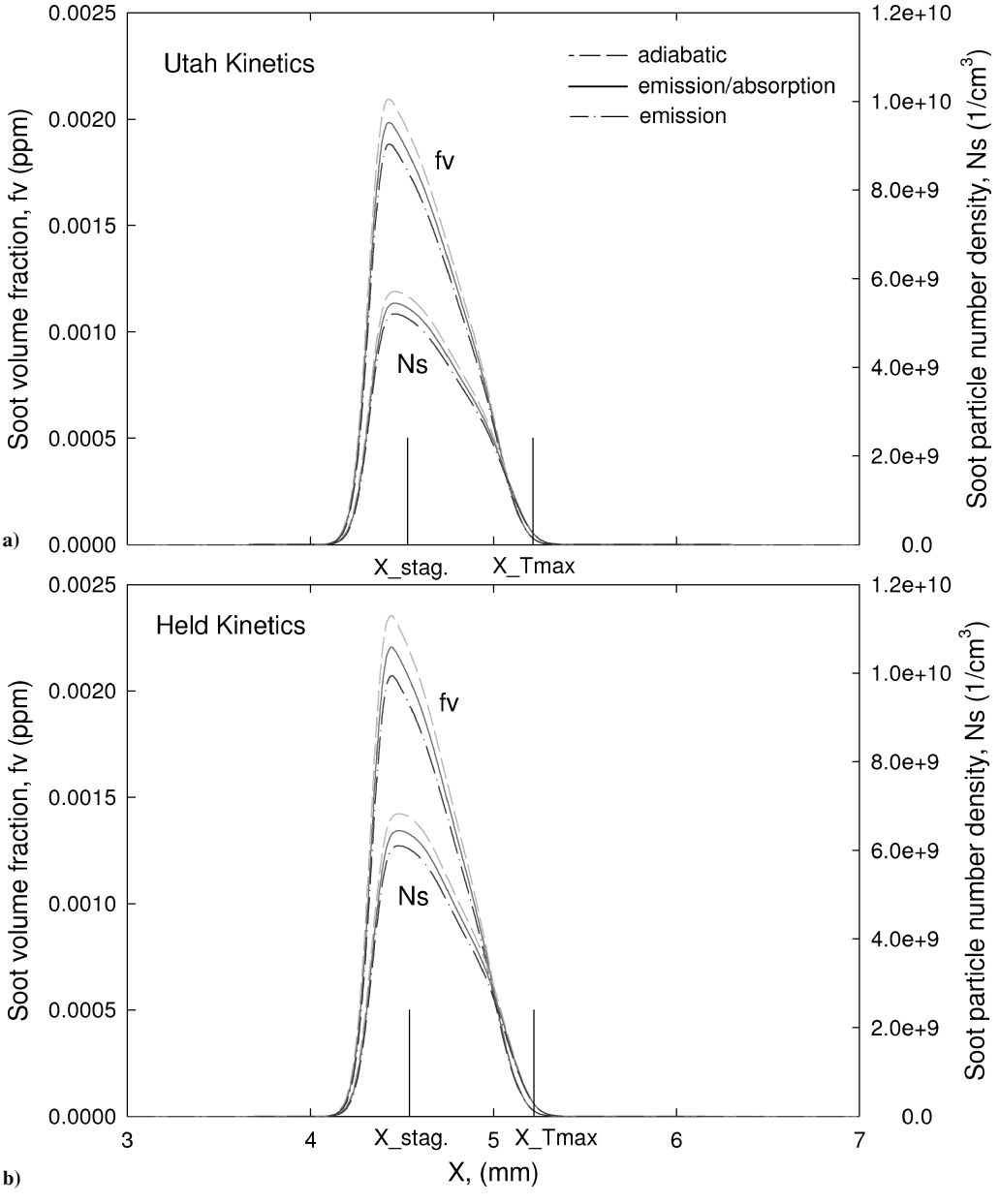

Fig. 3 Effects of radiation heat loss and chemical kinetics on soot volume fraction and number density distributions.

of these detailed reactions. Improved acetylene concentrations lead to better soot production estimation. More chemical reactions, up to PAH formation, should be included for high hydrocarbon fuel chemical kinetics, especially for strong sooting cases, even though it makes the calculation more complicated and time consuming.

Figure 3 shows the soot volume fraction f_v and number density N_s for Held's kinetics and University of Utah kinetics, with the three treatments of radiation. For the present flame, the soot particles are produced on the fuel side of the flame sheet, between the stagnation plane and the flame sheet, and transported toward the stagnation plane away from the flame. As the stagnation plane is approached, soot particle size increases by coagulation and surface growth of soot particles. The soot particles are transported across the stagnation plane toward the fuel side by thermophoresis. At the current conditions, the coagulation rate of soot number density is much lower on the fuel side of the main soot formation region. This leads to higher soot number density, even near the stagnation plane. The University of Utah heptane kinetics predicts lower soot density compared to Held's kinetics. The peak soot volume fraction is 11% lower for the adiabatic/emission case, due to the lower acetylene species concentration. Radiation affects the soot volume fraction, even for this low soot density case. By the use of the University of Utah heptane kinetics, the emission-only calculation yields a peak soot volume fraction that is 10% lower than that based on the adiabatic calculation. The effects of absorption lead to a 5.9% higher peak soot volume fraction for the emission/absorption case compared to the emission-only calculations.

Summary

The calculations by the use of both Held's and University of Utah kinetics show good agreement for heptane flames. However, the detail chemical mechanism for the high hydrocarbon radicals is important to accurately predict the high hydrocarbon species and then the soot formation. The detail chemical reactions including PAH formation are necessary for high hydrocarbon fuel chemical kinetics, especially for high sooting combustion. The radiation heat loss including emission and absorption from soot particles strongly affects the soot formation.

Acknowledgments

This work was supported by the U.S. Department of Energy (DOE) Direct Injection Engine Research Program at Sandia National Laboratory under Grant DE FG04 99AL66266, with B. Carling and J. Keller serving as DOE Scientific Officers. The authors fully acknowledge the contributions of T. J. Held and A. F. Sarofim, who provided the n-heptane mechanisms and advice regarding their use.

References

[1]Davis, S. G., and Law, C. K., "Laminar Flame Speeds and Oxidation Kinetics of iso-Octane–Air and n-Heptane–Air Flames," *Proceedings of the Combustion Institute*, Vol. 27, 1998, pp. 521–527.

[2]Seiser, R., Truett, L., Trees, D., and Seshadri, K., "Structure and Extinction and Non-Premixed n-Heptane Flames," *Proceedings of the Combustion Institute*, Vol. 27, 1998, pp. 649–657.

[3]Li, S. C., and Williams, F. A., "Counterflow Heptane Flame Structure," *Proceedings of the Combustion Institute*, Vol. 28, 2000, pp. 1031–1038.

[4]Held, T. J., Marchese, A. J., and Dryer, F. L., "A Semi-Empirical Reaction Mechanism for n-Heptane Oxidation and Pyrolysis," *Combustion Science and Technology*, Vol. 123, 1997, pp. 107–146.

[5]Chevalier, C., Pitz, W. J., Warnatz, J., Westbrook, C. K., and Melenk, H., "Hydrocarbon Ignition: Automatic Generation of Reaction Mechanisms and Applications to Modeling of Engine Knock," *Proceedings of the Combustion Institute*, Vol. 24, 1992, pp. 93–101.

[6]Bakali, A. E., Delfau, J., and Vovelle, C., "Kinetics Modelings of a Rich, Atmospheric Pressure, Premixed n-Heptane/O_2/N_2 Flame," *Combustion and Flame*, Vol. 118, 1999, pp. 381–398.

[7]Baek, S. W., Park, J. H., and Choi, C. E., "Investigation of Droplet Combustion with Nongray Gas Radiation Effects," *Combustion Science and Technology*, Vol. 142, 1999, pp. 55–79.

[8]Belardini, P., Dertoli, C., Beatrice, C., D'anna, A., and Giacomo, N. D., "Application of a Reduced Kinetic Model for Soot Formation and Burnout in Three-Dimensional Diesel Combustion Computations," *Proceedings of the Combustion Institute*, Vol. 26, 1996, pp. 2517–2524.

[9]Zhu, X. L., Kim, O. J., Frankel, S. H., Viskanta, R., and Gore, J. P., "Radiation Effects on Combustion and Pollutant Emissions," *Second Joint Meeting of the United States Sections of the Combustion Institute* [CD-ROM], Combustion Inst., Pittsburgh, PA, 2001.

[10]Lutz, A. E., Kee, R. J., Grcar, J. F., and Rupley, F. M., Sandia National Labs., Rept. SAND96-8243, Livermore, CA, 1997.

[11]Sarofim, A. F., and Zhang, H. R., "Numerical Combustion of Aviation Fuel Part I: A Cross-Model Comparison of n-Heptane Premixed Flame," *2003 Fall Meeting of the Western States Section of the Combustion Institute* [CD-ROM], Combustion Inst., Pittsburgh, PA, 2003.

[12]Fairweather, M., Jones, W. P., and Lindstedt, R. P., "Predictions of Radiative Transfer from a Turbulent Reacting Jet in a Cross-Wind," *Combustion and Flame*, Vol. 89, 1992, pp. 45–63.

[13]Sivathanu, Y. R., and Gore, J. P., "Coupled Radiation and Soot Kinetics Calculations in Laminar Acetylene/Air Diffusion Flames," *Combustion and Flame*, Vol. 97, 1994, pp. 161–172.

[14]Gore, J. P., Lim, J., Takeno, T., and Zhu, X. L., "A Study of the Effects of Thermal Radiation on the Structure of Methane/Air Counter-Flow Diffusion Flames Using Detailed Chemical Kinetics," *5th ASME/JSME Joint Thermal Engineering Conference* [CD-ROM], American Society of Mechanical Engineers, Fairfield, NJ, 1999.

[15]Crosbie, A. L., and Viskanta, R., "The Exact Solution to a Simple Nongray Radiative Transfer Problem," *Journal of Quantitative Spectroscopy and Radiative Transfer*, Vol. 9, 1969, pp. 553–568.

[16]Zhu, X. L., Gore, J. P., Karpetis, A. N., and Barlow, R. S., "The Effects of Self-Absorption of Radiation on Opposed Flow Partially Premixed Flame," *Combustion and Flame*, Vol. 129, 2002, pp. 342–345.

[17]Kim, O. J., Gore, J. P., Viskanta, R., and Zhu, X. L., "Prediction of Self-Absorption in Opposed Flow Diffusion and Partially Premixed Flames Using a Weighted Sum of Gray Gases Model (WSGGM)–Based Spectral Model," *Numerical Heat Transfer, Applications*, Vol. 44, 2003, pp. 335–353.

[18]Kim, O. J., Zhu, X. L., Viskanta, R., and Gore, J. P., "Prediction of Self-absorption of Radiation from Soot Particles in Opposed Flow Diffusion Flames," *Third Asia–Pacific Conference on Combustion*, Combustion Inst., Pittsburgh, PA, 2001, pp. 368–372.

C. Kaplan
Associate Editor

Comparing the *N*-Branch Genetic Algorithm and the Multi-Objective Genetic Algorithm

Eric T. Martin,* Rania A. Hassan,† and William A. Crossley‡
Purdue University, West Lafayette, Indiana 47907-1282

Nomenclature

c	=	penalty multiplier
E	=	material Young's modulus
f	=	fitness function
g	=	inequality constraint function
h	=	equality constraint function
J	=	number of inequality constraints

Received 10 February 2003; revision received 26 February 2004; accepted for publication 5 March 2004.

*Graduate Student, School of Aeronautics and Astronautics; currently Engineer, ATA Engineering, Inc., San Diego, CA 92130; eric.martin@ata-e.com.

†Graduate Student, School of Aeronautics and Astronautics; currently Postdoctoral Associate, Engineering Systems Division, Massachusetts Institute of Technology, Cambridge, MA 02139; rhassan@mit.edu. Member AIAA.

‡Associate Professor, School of Aeronautics and Astronautics, 1282 Grissom Hall; crossley@purdue.edu. Associate Fellow AIAA.